TISSUE ENGINEERING: Part A
Volume 22, Numbers 11 and 12, 2016

DOI: 10.1089/ten.tea.2015.0510

termis
Tissue Engineering
& Regenerative Medicine
International Society

ORIGINAL ARTICLE

Expandable Scaffold Improves Integration of Tissue-Engineered Cartilage: An *In Vivo* Study in a Rabbit Model

Chen-Chie Wang, MD, PhD,[1,2] Kai-Chiang Yang, PhD,[3] Keng-Hui Lin, PhD,[4] Yen-Liang Liu, MS,[5] Ya-Ting Yang, MS,[1] Tzong-Fu Kuo, PhD,[6] and Ing-Ho Chen, MD[2,7]

One of the major limitations of tissue-engineered cartilage is poor integration of chondrocytes and scaffold structures with recipient tissue. To overcome this limitation, an expandable scaffold with a honeycomb-like structure has been developed using microfluidic technology. In this study, we evaluated the performance of this expandable gelatin scaffold seeded with rabbit chondrocytes *in vivo*. The chondrocyte/scaffold constructs were implanted into regions of surgically introduced cylindrical osteochondral defects in rabbit femoral condyles. At 2, 4, and 6 months postsurgery, the implanted constructs were evaluated by gross and histological examinations. As expected, the osteochondral defects, which were untreated or transplanted with blank scaffolds, showed no signs of repair, whereas the defects transplanted with chondrocyte/scaffold constructs showed significant cartilage regeneration. Furthermore, the expandable scaffolds seeded with chondrocytes had more regenerated cartilage tissue and better integration with the recipient tissue than autologous chondrocyte implantation. Biomechanical tests revealed that the chondrocyte/scaffold group had the highest compressive strength among all groups at all three time points and endured a similar compressive force to normal cartilage after 6 months of implantation. Histological examinations revealed that the chondrocytes were distributed uniformly within the scaffolds, maintained a normal phenotype, and secreted functional components of the extracellular matrix. Histomorphometric assessment showed a remarkable total interface of up to 87% integration of the expandable scaffolds with the host tissue at 6 months postoperation. In conclusion, the expandable scaffolds improved chondrocyte/scaffold construct integration with the host tissue and were beneficial for cartilage repair.

Introduction

Cartilage has a low regenerative capacity and even minor trauma can result in progressive damage and degeneration. Autologous chondrocyte implantation (ACI) is an effective approach for the treatment of large full-thickness cartilage and osteochondral lesions with encouraging medium-term results.[1] However, repaired cartilage tissue in patients undergoing ACI has been shown to consist of a fibrocartilaginous matrix with abnormal collagen production.[2] Matrix-associated autologous chondrocyte implantation (MACI), which uses a cell carrier, is a new generation of cell therapy for cartilage repair.[3] A cell carrier, such as a fibrin clot, can improve the mechanical stability and durability of endogenous cells and provide proper stimulus for chondrogenic differentiation and cartilage regeneration.[4] The major limitation of the current MACI approach is inconsistent outcomes of the lateral integration between host and repaired tissues. Failure of cartilage integration, such as delamination, clefting, fracturing, and fissuring, at the boundary is commonly observed during MACI.

A chondrocyte/scaffold construct is a form of tissue engineering that is being increasingly used as an alternative approach for the repair of damaged cartilage.[5] In general, chondrocytes cultured in a monolayer manner can dedifferentiate and lose the chondrogenic phenotype.[6] However, it has been reported that

[1]Department of Orthopedic Surgery, Taipei Tzu Chi Hospital, The Buddhist Tzu Chi Medical Foundation, New Taipei City, Taiwan.
[2]Department of Orthopedics, School of Medicine, Tzu Chi University, Hualien, Taiwan.
[3]School of Biomedical Engineering, College of Biomedical Engineering, Taipei Medical University, Taipei, Taiwan.
[4]Institute of Physics and Research, Center for Applied Science, Academia Sinica, Taipei, Taiwan.
[5]Department of Biomedical Engineering, The University of Texas at Austin, Austin, Texas.
[6]Graduate Institute of Veterinary Medicine, School of Veterinary Medicine, National Taiwan University, Taipei, Taiwan.
[7]Department of Orthopedic Surgery, Hualien Tzu Chi Hospital, The Buddhist Tzu Chi Medical Foundation, Hualien, Taiwan.

these dedifferentiated cells are able to redifferentiate when chondrocytes are cultured in a three-dimensional (3D) microenvironment.[7,8] A 3D scaffold, which serves as a bioartificial extracellular matrix (ECM), has been shown to play a critical role in tissue engineering, with the raw material, architecture, and geometry of the scaffold modulating cellular behavior and ECM production.[9,10] In turn, the ECM has been shown to influence the function and phenotype of seeded cells, with cell attachment, migration, proliferation, and spatial arrangement being dramatically affected by the matrix composition and structure.[11]

Even though promising results of cartilage tissue engineering have been reported, problems such as inflammatory reactions to the implanted materials, poor cell-to-cell communication, toxic degradation products, and altered composition of the regenerated cartilage are concerns.[12–15] Another major concern is poor integration of the tissue-engineered cartilage with the host tissues. Indeed, gaps have been found between implanted chondrocyte/scaffold constructs and recipient tissue both in clinical trials and animal studies.[16,17] Trattnig *et al.* evaluated cartilage integration in humans using magnetic resonance imaging. Twenty patients were evaluated, of whom seven were defined as having poor or incomplete integration.[17] Thus, injectable hydrogel, which can be gelated *in situ* and used to fill the defect completely to avoid gaps in formation, is preferred as a scaffold. However, hydrogels are characterized by poor mechanical strength and are not able to sustain knee movements.

Recently, microfluidic technology has been used to develop an expandable scaffold with a highly ordered and uniform porous structure.[18] The expandable property of this scaffold may eliminate the formation of gaps between the engineered and host tissues. Moreover, chondrocytes seeded into this scaffold have been shown to maintain a functional phenotype *in vitro*. In the present study, we tested the *in vivo* performance of this expandable scaffold in a rabbit model of osteochondral defects.

Materials and Methods

Fabrication and characterization of the expandable scaffold

The expandable scaffold was prepared using the flow-focusing method with a microfluidic device.[18] Briefly, a gelatin solution (8%, A1890; Sigma-Aldrich) with a surfactant (0.5%, Pluronic® F127, P2443; Sigma-Aldrich) was pumped into the microfluidic device to generate equally sized microbubbles. The microbubbles were stored at −20°C for 30 min to allow for gelation, and then submerged in a 1% glutaraldehyde solution (G6257; Sigma-Aldrich) for cross-linking at 4°C for 12 h. The gelated closed cell construct was placed in a vacuum overnight to allow for formation of interconnected pores. The scaffold blocks were cut into uniform cylindrical scaffolds (3 mm in diameter and 3 mm in length) and stored in sterilized phosphate-buffered saline (PBS) containing 1% antibiotics at 4°C before use. To observe the architecture of the scaffold, fluorescein isothiocyanate (0.2 mg/mL, FITC, F7250; Sigma-Aldrich) was added to the gelatin solution. The fabrication of the gelatin scaffold was performed as previously described and inspected by a confocal laser scanning microscope (TCS-SP5; Leica).

The expandable scaffolds were dehydrated using absolute alcohol, and then immersed in distilled water to show the expansion capacity. A traditional gelatin scaffold was prepared using the freeze-dried method as a reference.[19] The expansion capacity of the expandable and freeze-dried gelatin scaffolds was evaluated based on the change in surface area measured by a ruler. The gap-filling capacity of the scaffolds was tested in plastic rings (5 mm cut from the edge of 0.2-mL Eppendorf tube) and 96-well tissue culture plates. An optical microscope and digital camera were used to record images.

Chondrocyte harvesting, culturing, and seeding into the scaffold

All experimental protocols and surgical procedures in the animal laboratory were approved by the Ethics Committee of Tzu-Chi General Hospital. New Zealand White rabbits, including cartilage donors and recipients, were housed in individual cages and allowed to move freely before the experiments. The animals were maintained in accordance with the International Council for Laboratory Animal Science guidelines for the care and use of laboratory animals. They were given tap water and food *ad libitum* and were acclimated for 14 days before the beginning of the experiments.

Six skeletally mature rabbits (age 10 weeks, mean weight 2280 ± 63 g) were sacrificed and served as the source of the chondrocytes. The thickness of these rabbits' knee joints (about 0.3 mm) is relatively thinner than other species (2.2–2.5 mm for humans, 0.4–0.5 mm for sheep, 0.6–1.3 mm for dogs, 0.7–1.5 mm for goats, and 1.5–2 mm for horses).[20] To minimize the number of animals used for chondrocyte isolation, we harvested articular cartilage tissues from the shoulder, hip, and stifle joints of the rabbits.[21] The pieces of cartilage were harvested from the joint surface using a scalpel. The slices of cartilage were washed with sterilized PBS, cut into thinner slices, and then immersed in 5% antibiotic solution for 15 min. After treatment, the cartilage slices were irrigated with PBS to remove residual antibiotics and then digested in 2% collagenase type II (C6885; Sigma-Aldrich) for 12 h. The digested cartilage was pelleted using centrifugation, resuspended in Dulbecco's modified Eagle's medium (DMEM, SH30003.01; Hyclone), and seeded into the culture dish at a cell density of 5×10^5 cells/mL. Chondrocytes were cultured in DMEM supplemented with 50 μg/mL L-ascorbic acid (A5960; Sigma-Aldrich), 10% fetal bovine serum (100–106; Gemini Bio-Products), and 1% antibiotics at 5% CO_2, 95% humidity, and 37°C. The medium was replaced every 2 days. The chondrocytes were examined regularly to ensure that fibroblastic transformation had not occurred.[22]

Cell seeding and cell/scaffold construct culturing

Chondrocytes (passage 3–5) were detached using trypsin-EDTA (15400; Gibco), resuspended in DMEM, and seeded into the gelatin scaffolds using a 24-gauge needle. Each scaffold contained 1×10^6 cells based on our previous *in vitro* study.[18] Cell/scaffold constructs were placed on a tissue culture plate for 1 h to allow for cell adhesion, and then culture medium was added. The cell/scaffold constructs were cultured in an incubator for another 24 h and then transplanted into the recipient rabbits.

Surgical implantation

A total of 18 rabbits (age 15 weeks, mean weight 3870 ± 21 g) were used as the recipients of the chondrocyte/scaffold constructs. Surgery was performed under general anesthesia through an intramuscular injection of Xylazine (5 mg/kg; Sun Star Chem & Pharm Corp.) with Zoletil (12.5 mg/kg; Virbace) in the lateral thigh. After skin preparation and sterilization, the right stifle joint was exposed by medial parapatellar arthrotomy, and the patella was subluxed to allow for full exposure of the stifle joint. Two osteochondral defects, 3 mm in diameter and 3 mm in height, were introduced in medial and lateral femoral condyles. The chondrocyte/scaffold constructs were implanted into the defect area over the medial femoral condyle (C + S group). No harvested periosteum or other commercial biological membrane was used to cover the implanted cell/scaffold constructs. Before implantation into the chondral defects, we used a dry gauze to gently remove liquid (culture medium) from the cell/scaffold constructs. The scaffolds had a high swelling ratio and porosity similar to a sponge. After implantation into the defects, the cell/scaffold constructs re-expanded due to the influx of fluid from bone marrow and joints and fit the chondral defect site firmly. The lateral femoral condylar defects were used as the control group.

In addition to the six rabbits in the control group at each time point, osteochondral defects were created in the contralateral legs as the experimental group. In the positive control group, the introduced defects received injections of allogeneic chondrocyte alone (allogeneic chondrocyte injection group).[23] Before injecting the cells, the outer surface of the defect was covered with one piece of periosteum harvested from the proximal tibia and sutured to the intact cartilage around the crater leaving one residual opening. After the cells had been injected into the osteochondral defects through the interstice, the crevice was sutured until the injection site was watertight. The experimental negative controls consisted of two groups; (1) in which the lateral osteochondral defects received a blank scaffold without cell seeding (S group); and (2) in which the defect was kept vacant *in situ* (Defect group). The incision was then closed with 5-0 Nylon sutures. Cephalosporin (25 mg/kg, Cefazolin sodium; Yung Shin) was injected intramuscularly in the lateral thighs to prevent postsurgical infections, and Fentanyl (Fentanyl citrate injection; Fresenius Bodene) was administered for pain control. The wounds were disinfected with beta-iodine once daily and kept dry with gauze and a bandage.

Gross observation and biomechanical testing of regenerated cartilage

Rabbits were sacrificed 2, 4, and 6 months after surgery. The gross morphology of the regenerated tissue was evaluated using the O'Driscoll score.[24] The distal medial femoral condyles containing the regenerated cartilage tissue were then retrieved using an oscillating saw. In preparation for the biomechanical tests, the samples were fixed in small plastic dishes. The dishes were mounted on a platform that enabled alignment of the cartilage surface perpendicular to an indenter probe.[25] The compressive strength of the retrieved tissue was assessed with an Instron 4505 mechanical tester. The biomechanical tests were performed in accordance with the guidelines in ASTM D5024-95a. Testing was performed in displacement controls with a speed set at 0.4 mm/min, and a 3-mm indenter was selected to match the dimensions of the specimens. Loading was applied until the specimens were compressed to $\sim 30\%$ of the original engineered cartilage thickness. Young's modulus was determined from the slope of the initial linear portion of the stress–strain curve. Unoperated rabbit lateral femoral condyles were used as normal controls.

Histologic examination and histomorphometric analysis

After the biomechanical tests, the samples were fixed in 10% neutral formalin for histological examinations. The osteotomized samples were then dehydrated in a graded series of ethanol and embedded in paraffin wax. Consecutive 5-μm-thick sections were then cut from the paraffin blocks. The sections were deparaffinized and stained with hematoxylin and eosin (H&E, 3008-1&3204-2; Muto) to assess the general construct morphology under an optical microscope (BX51; Olympus). Alcian blue staining (Muto) was used to evaluate glycosaminoglycan (GAG) production by the chondrocyte/scaffold constructs.

All histological stainings were assessed using histomorphometric analysis with ImageJ software (1.50a; Wayne Rasband). The entire length of the integration surface was traced manually and measured with the software. To evaluate the integration, the Repair Index evaluation methodology was used.[26] The quantification of the integration between the regenerated tissue and host cartilage was calculated and expressed as Disintegration (gap), Apposition (hypocellular or acellular zone), and Integration (no clear demarcation). Three interfaces were investigated in each sample. An unbound interface was defined as no bonding between the engineered cartilage and host tissue. A bonded interface was defined as the regenerated and surrounding tissues being in direct apposition, with a clear demarcation of the junction area being visible. An integrated interface was defined as a continuous interface of the engineered cartilage and host tissue without clear demarcation, cell migration to the junction, and good ECM remodeling.

Each histological section contained two interfaces; the left side was defined as Ax and the right as Ax + 1. All calculations were then performed using the following equations:

$$\%\ \text{Disintegration} = \frac{(A1 + A2)}{A} \times 100$$

A1 and A2 = unbound interface (length, μm), A = total interface of both sites (μm).

$$\%\ \text{Apposition} = \frac{(A3 + A4)}{A} \times 100$$

A3 and A4 = bonded interface (length, μm)

$$\%\ \text{Integration} = \frac{(A5 + A6)}{A} \times 100$$

A5 and A6 = integrated interface (length, μm)

Immunohistochemical staining

The expression of type I, type II, and type X collagens and S-100 was analyzed using immunohistochemical staining. The sections were baked at 56°C for 10 min, deparaffinized, rehydrated, enzymatically pretreated for antigen retrieval, immersed in PBS with 3% H_2O_2 for 20 min to quench the endogenous peroxidase activity, and preincubated with serum blocking solution for 60 min to block the nonspecific binding before application of the primary antibodies. The sections were pretreated with pronase (1 mg/mL in pH 7.6 Tris buffer for 15 min at 25°C, SI-P5147; Sigma-Aldrich) for type I collagen staining, pepsin (4% in 0.01 N HCl for 10 min at 37°C, P-7000; Sigma-Aldrich) for type II collagen staining, pepsin (1 mg/mL in 0.1N HCl for 2 h at 37°C) and hyaluronidase (10 mg/mL in PBS for 30 min at 37°C, SI-H3884; Sigma-Aldrich) for type X collagen staining, and hyaluronidase (2 mg/mL in pH 5.0 PBS for 60 min at 37°C) for S-100 staining. The sections were incubated with anti-type I collagen antibodies (1:500, bs-0578R; Bioss), anti-type II collagen antibodies (1:200, bs-0709R; Bioss), or S-100 antibodies (1:500, bs-1248R; Bioss) at 4°C overnight. For anti-type X collagen antibodies, the sections were incubated with anti-type X collagen primary antibodies (1:2000, ab49945; Abcam) at room temperature for 1 h. The staining on the slides was developed using 3, 3′-diaminobenzidine (Super Sensitive™* Polymer-HRP Detection System; BioGenex). The sections were counterstained with Mayer's hematoxylin. Negative controls were processed identically, except that the primary antibodies were replaced with IgG.

Statistical analysis

The data obtained are expressed as mean ± standard error of the mean. One-way analysis of variance analysis with *post hoc* Dunnett's multiple comparison tests was used to analyze the differences between groups. A difference was considered statistically significant if the p-value was smaller than 0.05.

Results

Characterization of the expandable scaffold

The microbubbles self-assembled layer by layer, reconstituting a highly organized 3D ordered array with a highly organized honeycomb-like structure (Fig. 1a). An interconnecting porous structure was found in the gelatin scaffold under confocal microscopy.

The expansion abilities of the expandable and freeze-dried gelatin scaffolds were determined based on changes in the surface area. The expandable scaffolds had a significantly higher expansive capacity (2.64 ± 0.15-fold increase in surface area, $p < 0.01$, Fig. 1c) compared with the freeze-dried scaffolds (1.87 ± 0.08-fold, Fig. 1b). The test using plastic rings from Eppendorf tubes and 96-well plates further supported this finding (refer to the Materials and Methods section). When freeze-dried scaffolds were rehydrated, minor gaps were found between the scaffolds and the walls of the tubes or wells (Fig. 1b). In contrast, the expandable scaffolds fit the wells or plastic rings completely, with no evidence of gap formation (Fig. 1c).

Clinical evaluation

All rabbits regained motility on the second day post-surgery. Wound healing was monitored for 1 week, after which the sutures were removed. No wound infection or dehiscence was observed, and the gait pattern returned to preoperative status. One animal in the allogeneic chondrocyte injection group died suddenly due to rhinorrhea lasting for 2 days caused by an upper airway infection. An autopsy confirmed the absence of septic arthritis in the experimental stifle joint. This animal was excluded from the study and replaced with a new animal.

Gross morphology

The rabbits were sacrificed 2, 4, and 6 months postoperatively. After arthrotomy of the stifle joint, no obvious adhesive arthritis, infection, or inflammatory synovitis was detected. Marginal osteophytosis over lateral femoral condyles was found in three animals (one in the S group and two in the Defect group at 6 months postoperatively). Careful inspection and evaluation of all defects in the experimental and positive/negative control groups were carried out after opening the joint cavities (Fig. 2). After 2 months, macroscopic investigation revealed that all defects were filled with varying amounts of regenerated tissue of variable color (white, grayish, and beige) in all of the groups.

In the C + S group, all defects were filled with white tissue and matched the original contour of the medial femoral condyle. The color of the regenerated tissue was more transparent compared with the surrounding host cartilage. An apparent whiter ring surrounding the regenerated tissue was in tight contact with the inner edge of the recipient cartilage with no visible crevices. In some cases, the color of the regenerated tissue was the same as the color of the host cartilage with no obvious demarcation. In general, the implant site of the experimental group was completely filled at all time points. Macroscopically, the regenerated cartilage became whiter, less transparent, and more similar to adjacent tissues at later time points. The whiter ring surrounding the regenerated tissue that was apparent at the 2-month time point had almost disappeared in the 4- and 6-month groups.

In the allogeneic chondrocyte injection group, the chondral defects were not completely filled with new tissue even after 6 months. Residual defects were mostly observed in the upper corners of the created cylindrical craters. The color of the regenerated tissue was white, with a transparency similar to the adjacent host cartilage. Less tissue was formed in the animals that received a blank scaffold (S group) compared with those in the C + S and allogeneic chondrocyte injection groups at all time points. The defects were still dented, and somewhat irregular, white cartilage-like tissue was observed only at the bottom of the defects. In the chondral Defect group, depressions were still observed after 2 months, and after 6 months, marginal osteophytosis was apparent. Residual healthy cartilage appeared to be worn out and some fissuring was observed.

O'Driscoll score and histological assessment

The regenerated cartilaginous tissues in the femoral condyles were further assessed using the O'Driscoll scoring

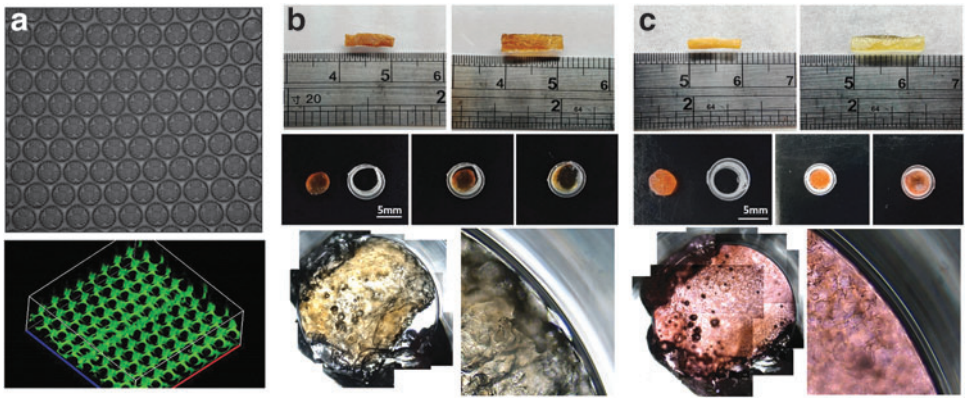

FIG. 1. **(a)** The microbubbles were reconstituted as a highly organized three-dimensional ordered array structure. An interconnecting porous structure was observed under confocal microscopy. The expansion capacity of the expandable and freeze-dried gelatin scaffolds was measured in an Eppendorf tube (*upper panel*) or a 96-well plate (*lower panel*). **(b)** The surface area of the freeze-dried gelatin scaffold expanded by 1.87 ± 0.08-fold after immersion in distilled water. Rehydrated freeze-dried scaffolds demonstrated minor gaps between the scaffold and the walls of the tubes. **(c)** Rehydration of the expandable gelatin scaffold showed a 2.64 ± 0.15-fold increase in surface area. In comparison with the freeze-dried scaffolds, the expandable scaffolds fitted the wells completely with no evidence of gaps. Color images available online at www.liebertpub.com/tea

system (Table 1). Compared with the Defect and S groups, the allogeneic chondrocyte injection and C+S groups showed significant improvement indices ($p < 0.05$) at 2 months postoperation (post-OP). There were no significant differences between the allogeneic chondrocyte injection and C+S groups at this time point. There were no improvements in the indices in the Defect, allogeneic chondrocyte injection, and S groups at 4 months post-OP compared with 2 months post-OP. The allogeneic chondrocyte injection group still had a significantly higher index compared with the Defect and S groups ($p < 0.05$) at 4 months post-OP. Remarkably, the O'Driscoll index continued to improve in the C+S group at 4 months and was the highest among all groups at this time point. At 6 months post-OP, the allogeneic chondrocyte injection group had a significantly higher index than the Defect and the S groups ($p < 0.05$), and the C+S group still had the highest index among all groups. The O'Driscoll score suggested that the

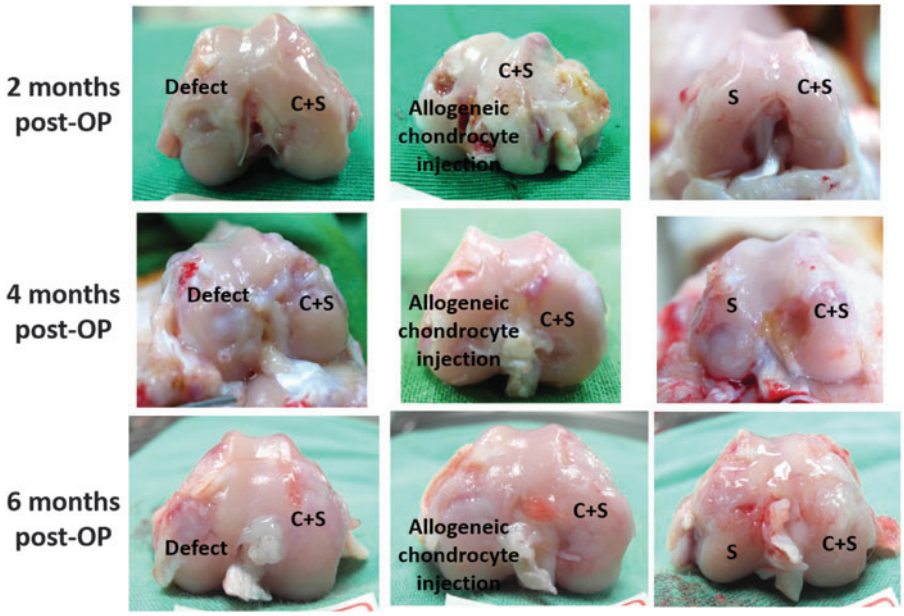

FIG. 2. Gross morphology of a rabbit knee postoperatively. After 2 months, macroscopic analysis revealed that all defects had been filled with varying amounts of regenerated tissue. In the C+S group, all of the defects were filled with white tissue that matched the original contours of the medial femoral condyle. A discernible whiter ring was noted between the regenerated tissue and recipient cartilage. The surrounding ring had almost completely disappeared after 4 and 6 months. In the allogeneic chondrocyte injection group, the chondral defects were not completely filled with new tissue even after 6 months. For the animals in the S group, the defects were still dented with somewhat irregular, white cartilage-like tissue only at the bottom of the defects. In the Defect group, the depressions were still observed after 2 months. Color images available online at www.liebertpub.com/tea

Table 1. Mean Histological Scores Assessed by Modified O'Driscoll Scoring System (Maximum Score = 23) for the Gelatin Microfluidic Scaffold in Full-Thickness Chondral Defects

Months	*Defect*	*Allogeneic chondrocyte injection*	*S*	*C+S*
2	5±3	11±2[a,b]	7±2	14±1[a,b]
4	6±2	13±1[a,b]	8±1	17±2[a–c]
6	9±3	14±3[a,c]	10±2	19±3[a–c]

Defect: empty defect without further treatment; Allogeneic chondrocyte injection: allogeneic chondrocyte implantation with periosteum covered; S: scaffold only; C+S: chondrocytes + scaffold.
[a]Significant difference when compared with the index of Defect group.
[b]Significant difference when compared with the index of allogeneic chondrocyte injection group.
[c]Significant difference when compared with the index of S group.

cell/scaffold constructs enhanced cellular ingrowth and the amount of hyaline cartilage-like tissue.

Cartilage tissue repair at 2 months post-OP

Histological inspection of the joint sections revealed that the introduced defects treated with the chondrocyte/scaffold constructs (C + S group) were filled with cartilage-like tissue after 2 months (Fig. 3). The surface of the defects was smooth with no visible gaps between the transplanted and host tissues. In addition, the regenerated tissue was positive for type II collagen and S-100, but only weak positive for type X collagen. The tissues that were positive for type I collagen were located in the subchondral bone. Hence, the regenerated tissue had a remarkable resemblance to the cartilage tissue.

In the allogeneic chondrocyte injection group, a greater tissue response was detected over the deep portion of the introduced defect and surrounding area. These new matrices were barely populated with cells and formed an inclination from the surface cliff of the host cartilage to the bottom of the crater. The defects were still devoid of newly formed tissue, and the contours of the defects displayed central saucer-shaped depressions. The regenerated tissue consisted of cartilage-like tissue, with an appearance of a mixture of hyaline cartilage and fibrocartilage. The fibrocartilage-like tissues expressed both type I and type II collagens. The hyaline cartilage-like tissue was mainly located at the border of the host cartilage and the base of the created defect. Peripheral fissures were also found in this group.

Smaller round chondrocytes were present at the interface between the implanted scaffold and the host bone in the basal areas of the defects in the allogeneic chondrocyte injection group. These chondrocytes resembled hypertrophic chondrocytes, which cause enchondral calcification. In some cases, bone growth was observed on the matrix fibers.

In the Defect group, considerable subchondral tissue response and partially remodeled subchondral bone were observed in the rim of the basin. The superficial area of the newly regenerated tissue mainly consisted of fibrous or fibrocartilaginous tissues, and these tissues had a low expression of type II collagen, but high expression of type I and type X collagens.

Cartilage tissue repair at 4 months post-OP

At 4 months postsurgery, the implanted scaffolds had almost completely degraded, and the boundaries of the microbubbles were not visible in the C + S and S groups (Fig. 4). In some defects in the C + S group, the repaired tissue was slightly overgrown in comparison with the adjacent host cartilage and relatively light. Relative lighter staining with Alcian blue and surface fibrillation were also observed in the superficial area of the defects. Integration with no visible gaps between the engineered cartilage and the host tissue was observed in all animals in the C + S group. Remodeling of the subchondral bone was complete and consistent with the host bone. Immunohistochemical staining revealed that the regenerated tissues produced ECM proteins at normal levels.

The superficial area of the defects treated with allogeneic chondrocyte injections was replaced with fibrocartilaginous tissue that strongly expressed type I collagen. Continuity between the regenerated tissue and the host cartilage was observed occasionally, and gaps were obvious. Surface delamination and fibrillation were also noted. Dimpling of the surface was observed in most cases.

In the S group, the repaired tissue had a fibrocartilage-like appearance with loose ECM and poor GAG production. In most cases, the introduced defects still possessed a central depression, which was deeper compared with the allogeneic chondrocyte injection group. Deep fissures were also apparent at the interface between the regenerated tissue and the host cartilage.

In the Defect group, repaired tissue was found in the peripheral region and it had a fibrocartilage-like appearance. Alcian blue staining was significantly lighter in comparison with the adjacent host cartilage. Surface fibrillation was noted in most specimens.

Cartilage tissue repair at 6 months post-OP

In the C + S group, the regenerated cartilage showed good surface continuity, and the tidemark was reconstructed through idoneous subchondral bone remodeling (Fig. 5). The introduced defects were filled with full-thickness regenerated hyaline cartilage tissue that expressed GAGs. The junction between the repaired and the host cartilage revealed good continuity with optimal cell growth and ECM secretion. In the junction, the cells were loosely distributed, which mimicked the scattered chondrocytes in the hyaline cartilage. No obvious transitional zone was observed between the engineered and the host cartilage.

In the allogeneic chondrocyte injection group, the defects were repaired with a mix of fibrocartilage and hyaline cartilage-like tissues. Superficial layer fibrillation and delamination were observed in most cases compared with the results at 4 months in the allogeneic chondrocyte injection group, which suggested degeneration of the regenerated cartilage. Hypocellularity in the junction area and chondrocyte cluster formation near the regenerated cartilage also suggested ongoing degeneration of the cartilage.

In the S and Defect groups, central depression, superficial fibrillation, clefting, and deep fissures that reached subchondral bone were observed. The regenerated fibrocartilage or fibrous tissue appeared to be hypocellular with a disorganized ECM structure, and this was especially pronounced in the S group. In

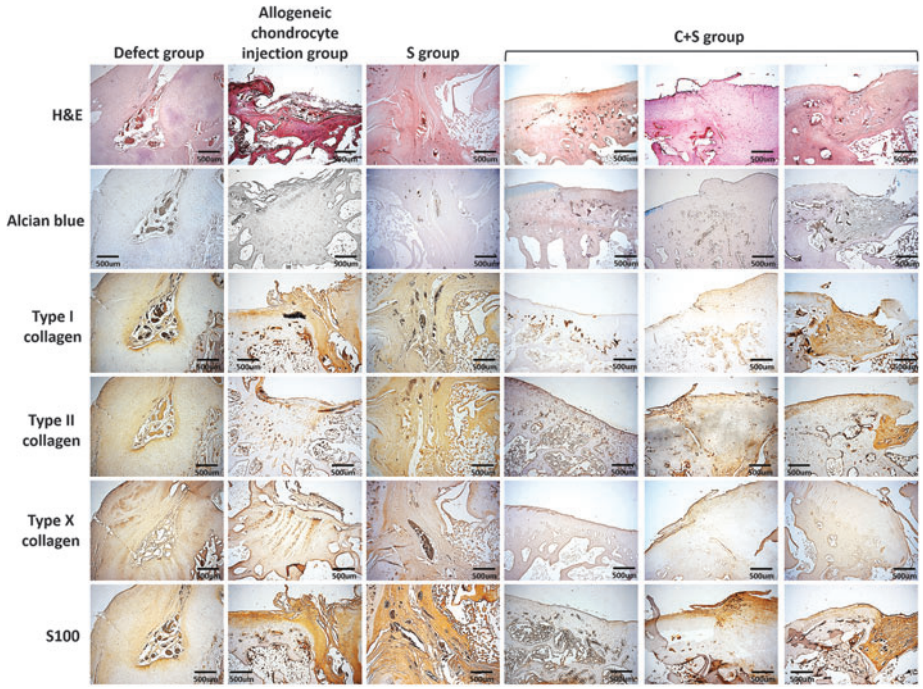

FIG. 3. Histological evaluation of regenerated cartilage at 2 months post-OP. H&E staining of regenerated tissues revealed that the created defects treated with the cell/scaffold constructs (C + S group) were almost completely filled with hyaline cartilage-like tissue. In the allogeneic chondrocyte injection group, the regenerated tissue consisted of cartilage-like tissue, with the appearance of hyaline cartilage with fibrocartilage interposition. In the S group, some new tissue had formed near the host cartilage. The Defect group showed some fibrous tissue formation in the defects. The C + S group showed a homogeneous Alcian bluish hue. Intervenient Alcian blue staining indicated a mixture (fibrocartilage and hyaline cartilage) of regenerated tissues in the allogeneic chondrocyte injection group. Light blue staining was seen in the Defect group. Positive type II collagen staining was observed in the C + S group in the regenerated and host cartilage. Type II collagen was mainly expressed at the border of the host cartilage and the base of the created defect in the Defect group. Scale bar = 500 μm.

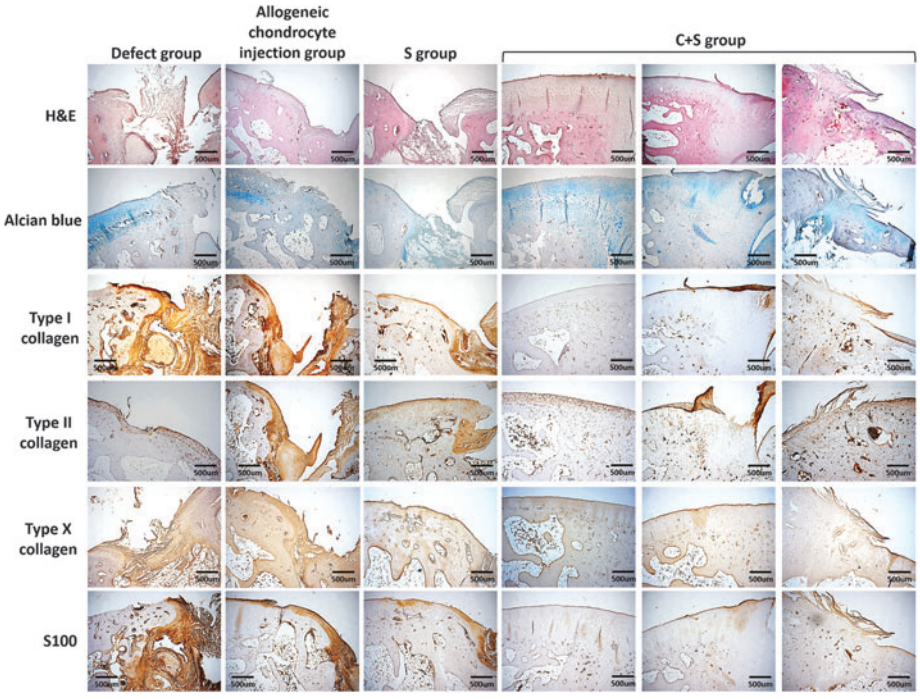

FIG. 4. Histological evaluation of the regenerated cartilage at 4 months post-OP. The created defects were only partially filled with new tissue; however, the volume of the regenerated tissue had increased at 4 months post-OP in the allogeneic chondrocyte injection group. Weak or negative type I collagen staining was observed in the C + S group. Persistent positive type I collagen staining was observed in the regenerated tissue surrounding the treated defect in the Defect and S groups. No expression of type X collagen was detected at 4 and 6 months post-OP in the C + S group. Scale bar = 500 μm. post-OP, post-operation.

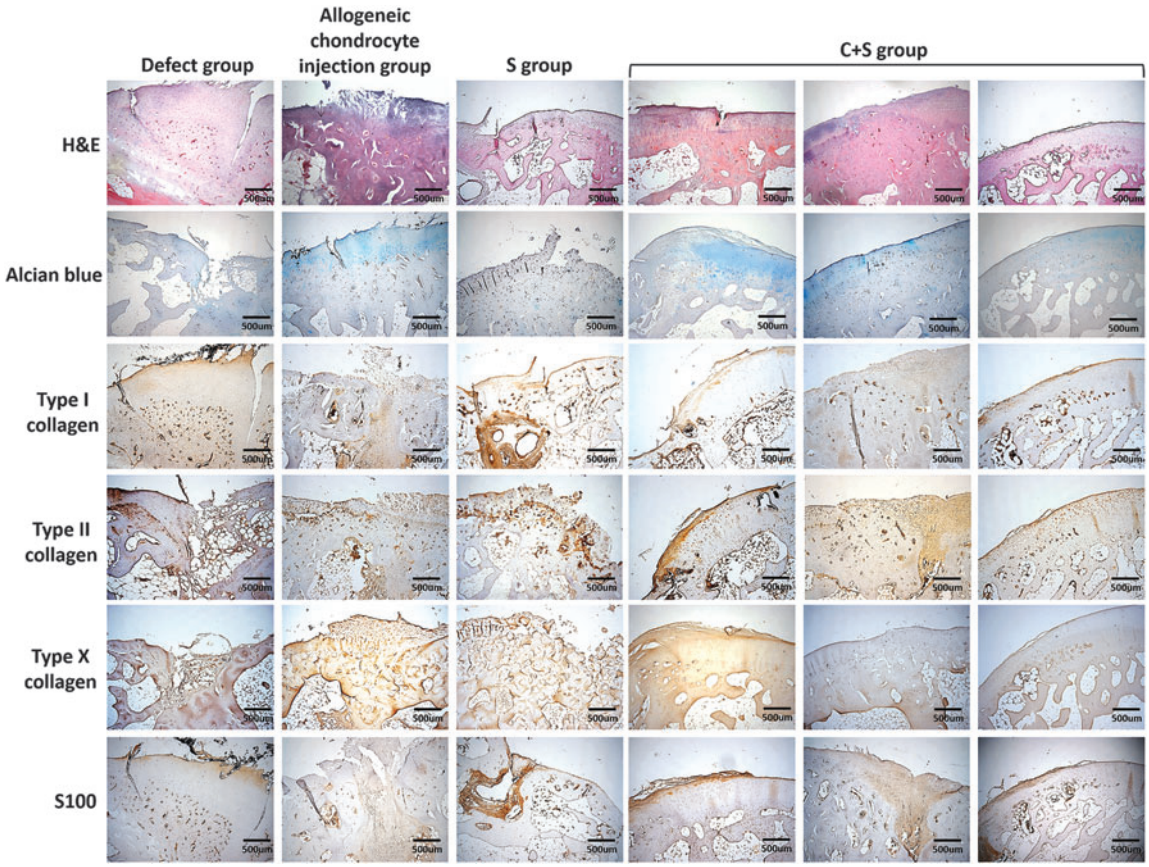

FIG. 5. Histological evaluation of the regenerated cartilage at 6 months post-OP. H&E staining revealed that the regenerated cartilage had good surface continuity and idoneous subchondral bone remodeling at 6 months post-OP in the C + S group. Alcian blue staining for GAG production showed strong bluish staining at 6 months post-OP in the C + S group. In the allogeneic chondrocyte injection group, type X collagen was strongly expressed at 2 and 4 months post-OP, and then decreased by 6 months post-OP. Positive type X collagen staining was observed at all time points in the S and Defect groups. In the C + S group, repaired tissues displayed high S-100 staining that gradually increased until 6 months post-OP. Scale bar = 500 μm. GAG, glycosaminoglycan; H&E, hematoxylin and eosin.

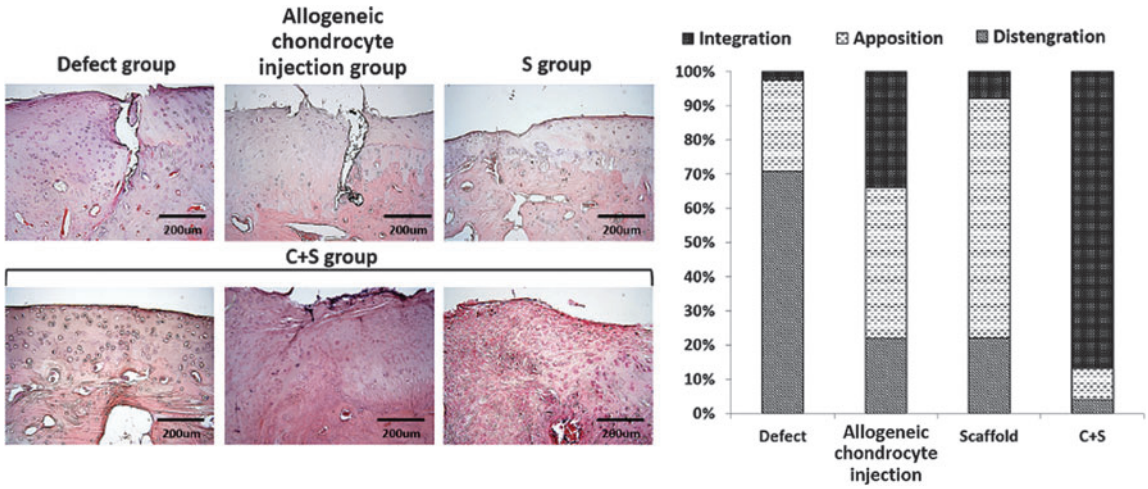

FIG. 6. Histomorphometric evaluation of the regenerated cartilage. In the C + S group, excellent integration of up to 87% of the total interface was observed. In addition, no obvious demarcation such as hypocellularity or gap formation was detected in this group. The integration ratios in the allogeneic chondrocyte injection, S, and Defect groups were 34%, 8%, and 2.5%, respectively. All groups displayed varying degrees of apposition. In the C + S group, disintegration was significantly lower than in the other three groups and accounts for 4% of the interface. Scale bar = 200 μm. Color images available online at www.liebertpub.com/tea

addition, immunohistochemical analysis showed abnormal protein production in the regenerated tissue in these two groups.

Histomorphometric assessment

Excellent integration with up to 87% of the total interface (Fig. 6) and absence of obvious demarcation such as hypocellularity or gaps were observed in the C + S group. The integration ratios in the allogeneic chondrocyte injection, S, and Defect groups were 34%, 8%, and 2.5%, respectively. All groups displayed varying degrees of apposition, with the highest degree in the S group. The Defect group displayed a somewhat lower apposition of 27%. The highest level of disintegration (71% of the total interface) was observed in the Defect controls group, and the smallest disintegration level of 4% of the interface was observed in the C + S group. The disintegration rate in the C + S group was significantly lower than in other three groups.

Compression strength

At 2 months post-OP, the compressive strength of the C + S group was significantly higher compared with the Defects group ($p < 0.01$), allogeneic chondrocyte injection group ($p < 0.05$), and S group ($p < 0.05$, Table 2). There was no significant difference between the allogeneic chondrocyte injection and S groups; however, the C + S group still had significantly lower compressive strength compared with intact cartilage ($p < 0.01$). At 4 months post-OP, the allogeneic chondrocyte injection group had significantly higher compressive strength compared with the Defect and S groups (both $p < 0.05$). No significant differences were found between the Defect and S groups. The C + S group had the highest compressive strength among all groups ($p < 0.05$ vs. the allogeneic chondrocyte injection group, $p < 0.01$ vs. the Defect and S groups), although it was still significantly lower than health cartilage ($p < 0.05$). At 6 months post-OP, the C + S group had the highest compressive strength relative to the other three groups ($p < 0.01$ vs. the Defect and S groups, and $p < 0.05$ vs. the allogeneic chondrocyte injection group). No significant difference between the C + S group and normal cartilage group was noted, indicating that the stiffness of the regenerated tissue in the C + S group was similar to normal cartilage after 6 months of implantation.

Discussion

Integration of the chondrocyte/scaffold constructs with the host tissue is a critical issue for tissue-engineered cartilage. Intrinsic factors that influence cartilage integration include chondrocyte dedifferentiation, cell apoptosis, cell hypertrophy, the nature of regenerated ECM, the cells used to repopulate the chondral defects, and the type of biomaterial scaffold used in the repair. Since all of these issues are influenced by the properties of the scaffold, research to improve the scaffold design is important.

In this study, we describe a repair process that takes place at the interface between host tissue and expandable tissue-engineered cartilage *in vivo*. The highest integration was observed in the C + S group at 4 months post-OP, with the tidemark being reconstructed through subchondral bone remodeling at 6 months post-OP. An increase in the compressive strength in the C + S group over a 2-month period was observed, and this strength had further increased at 4 months post-OP. However, the compressive stiffness of the regenerated tissue in the C + S group achieved a comparable level with normal cartilage up to 6 months of implantation. These results indicate that the engineered cartilage in this rabbit model needed 6 months to achieve histological organization and biomechanical stiffness in the process of cartilage maturation.

Several previous studies have also focused on enhancing tissue-engineered cartilage integration. Pabbruwe *et al.* investigated the effects of a collagen membrane scaffold on cartilage integration.[27] In their study, chondrocytes were seeded onto both surfaces of a collagen membrane scaffold and then placed between two cartilage discs. The use of this scaffold resulted in a higher histomorphometric repair index and better tensile strength compared with the control groups (allogeneic chondrocyte injection group or scaffold only). However, since most chondral lesions are larger than a cartilage fissure, membrane-like scaffolds are not clinically suitable for this kind of repair. Peretti *et al.* conducted a series of studies using cartilage/devitalized-cartilage matrix/cartilage sandwich models to investigate cartilage integration.[28] The combined structure was implanted into a subcutaneous pouch on the back of nude mice. The level of integration of the experimental construct was assessed, and continuous remodeling of the newly formed matrix was observed. The disadvantage of this composite construct is its substantial thickness and lack of flexibility needed to fill in small gaps between two cartilage surfaces. Another study used highly purified collagenase VII and hyaluronidase to eliminate devitalized chondrocytes and tissue from the wound edge, which led to living cells accumulating in the wound area after treatment.[29] Good cartilage integration was noted in both bovine and human models *in vitro* when this approach was used. The rationale behind this method is the elimination of the inhibitory effects of deteriorated tissue on tissue regeneration. However, this approach has limitations with regard to *in vivo* and clinical applications as enzymes may leak into the joint cavity and pose a hazard for adjacent tissues.

Another study reported a biphasic scaffold consisting of collagen gel overlying a tricalcium phosphate block, which

Table 2. Compression Strength (MPa) of Regenerated Cartilage Tissues

Months	*Defect*	*Allogeneic chondrocyte injection*	*S*	*C + S*	*Control*
2	0.18 ± 0.12	0.28 ± 0.08	0.22 ± 0.13	0.41 ± 0.12	0.89 ± 0.13
4	0.25 ± 0.13	0.35 ± 0.17	0.27 ± 0.12	0.59 ± 0.09	
6	0.28 ± 0.11	0.46 ± 0.12	0.32 ± 0.09	0.83 ± 0.16	

Control: intact cartilage.

was implanted into rabbit femoral trochlear groove defects.[30] After 12 weeks of implantation, the regenerated tissue revealed abundant hyaline-like cartilage; however, degenerated cartilage was gradually noted with time. At 30 weeks, 76% of the repaired tissues were fibrous tissue and fibrocartilage. The possible reason for the cartilage degeneration was attributed to poor biomechanical stiffness compared with adjacent normal cartilage, and this may have been due to the inherently lower stiffness of the collagen gel component of the biphasic scaffold. In the current study, the biomechanical test results revealed that the chondrocyte/scaffold constructs had comparable strength with the normal cartilage after 6 months of implantation. This may be because our scaffold was a highly organized honeycomb-like hexagonal stacking structure with stronger mechanical properties compared with a hydrogel.[18] The higher stiffness of our scaffold may have been present in the implanted site for a longer period of time. Another possible reason for the biomechanical results in our *in vivo* study is that our scaffold had a higher porosity and swelling ratio. These two characteristics can lead to cell migration into deeper portions of the scaffold and maintain cell vitality. More surviving cells can then secrete more ECM to further support the structure of the scaffold and help maintain enough mechanical support for the newly regenerated cartilage.

The expansion capability of our microfluidic scaffold underlies its excellent adherence to surrounding tissue. The existing dented and scratched areas were fully filled by the expanded portion of the scaffold, which resembled branching tentacles. The resulting blocking mechanism is similar to the locking of a cog wheel, which is molded to a matching shape. Viscosity of the gelatin strengthens the interactions between the scaffold and host tissue and is another reason for the superb adhering characteristics of our scaffold. Many methods using scaffolds and ACI such as Carticel require the use of the periosteum to cover the implant to prevent its dislodging.[31] The chondroprogenitor cells that populate the cambium layer of the periosteum may migrate into the scaffold and proliferate there. This complicates the identification of the cell source during assessment of cartilage regeneration. Our scaffold does not need to be covered with periosteum, is easily mounted into a defect, and can be evaluated without possible contamination issues. Another advantage of our scaffold is the good hemostasis property of gelatin.[32,33] Lesser blood loss favors less tissue inflammation, thereby shortening the time required for postoperative recovery.

In addition, our scaffold has extremely high extensibility. The surface of the osteochondral defects created in this study had microscopic scratches and dents. Such irregularities prevent perfect contact between the engineered scaffolds and the inner wall of the defects, despite the size-matching construction. Our scaffold could fill any gaps and demonstrated locomotion similar to the pseudopodium of some microorganisms. The ability to fill such gaps was due to the high swelling ratio and porosity. In our previous *in vitro* study, we showed that both swelling ratio and porosity of an expandable scaffold were dramatically higher than in a freeze-dried scaffold.[18] Gelatin hydrophilicity and the hexagonal structure of the stacking bubbles were most likely responsible for the excellent extensibility of this microfluidic scaffold. Gelatin contains a large number of hydroxyl, carboxyl, and amino groups and therefore is highly hydrophilic. Scaffolds with higher hydrophilicity have been shown to possess a higher swelling ratio and extension ability.[12,34] The stereoscopic expansible microstructure of the scaffold allows it to fill the pits and gaps between host tissue and engineered cartilage. Furthermore, a highly abundant RGD sequence, which is a characteristic of our gelatin scaffold, may be another reason for the high integration properties. An RGD sequence has been shown to improve cell attachment and thus may aid in cartilage integration.[35] Taken together, the benefits of our scaffold for cartilage tissue engineering suggest its suitability for clinical application.

A limitation of this study is that different locations of cell/scaffold implantation may have confounded the repair quality of regeneration of the engineered cartilage.[36] For example, the femoral trochlea is a nonweight-bearing area and only receives the patellar reaction force. Thus, engineered cartilage implanted into this portion will have better results than in medial or lateral femoral condyles. Another limitation is the short period of post-OP follow-up of only 6 months. As cartilage degeneration is associated with aging, further studies over the whole life span of a rabbit may be warranted.

Conclusions

The high porosity and swelling ratio of our expandable scaffold resemble the ultrastructure of normal cartilage. In addition, the high extensibility of our scaffold greatly improved surface contact between the regenerated cartilage and host tissue. Our results demonstrated that this expandable scaffold had high integration efficiency, and the chondrocytes within the scaffold possessed a normal phenotype with adequate ECM production. Biomechanical tests revealed that the chondrocyte/expandable scaffold constructs had the highest compressive strength than the other groups at all three time points and endured a similar compressive force to normal cartilage after 6 months of implantation. These promising and exciting results warrant long-term follow-up experiments and large animal studies to further assess the biocompatibility and longevity of this expandable scaffold.

Acknowledgments

This research was supported by the National Science Council, Taiwan, under Grant NSC102-2320-B-303-001-MY3 and Tzu-Chi General Hospital under Grant TCRD-I104-02-02. The authors would like to thank Hae-Wen Tzou (Central laboratory at National Taiwan University and Taipei Tzu-Chi General Hospital) for assistance with animal studies and histological staining evaluation.

Disclosure Statement

No competing financial interests exist.

References

1. Harris, J.D., Siston, R.A., Pan, X., and Flanigan, D.C. Autologous chondrocyte implantation: a systematic review. J Bone Joint Surg Am **92,** 2220, 2010.

2. Roberts, S., Hollander, A.P., Caterson, B., Menage, J., and Richardson, J.B. Matrix turnover in human cartilage repair tissue in autologous chondrocyte implantation. Arthritis Rheum **44,** 2586, 2001.
3. Brittberg, M. Cell carriers as the next generation of cell therapy for cartilage repair: a review of the matrix-induced autologous chondrocyte implantation procedure. Am J Sports Med **38,** 1259, 2010.
4. Gille, J., Behrens, P., Volpi, P., de Girolamo, L., Reiss, E., Zoch, W., *et al.* Outcome of Autologous Matrix Induced Chondrogenesis (AMIC) in cartilage knee surgery: data of the AMIC Registry. Arch Orthop Trauma Surg **133,** 87, 2013.
5. Demoor, M., Ollitrault, D., Gomez-Leduc, T., Bouyoucef, M., Hervieu, M., Fabre, H., *et al.* Cartilage tissue engineering: molecular control of chondrocyte differentiation for proper cartilage matrix reconstruction. Biochim Biophys Acta **1840,** 2414, 2014.
6. Yang, K.C., Wu, C.C., Chen, W.Y., Sumi, S., and Huang, T.L. L-Lysine regulates tumor necrosis factor-alpha and matrix metalloproteinase-3 expression in human osteoarthritic chondrocytes. Process Biochem [Epub ahead of print]; DOI: 10.1016/j.procbio.2016.04.009.
7. Benya, P.D., and Shaffer, J.D. Dedifferentiated chondrocytes reexpress the differentiated collagen phenotype when cultured in agarose gels. Cell **30,** 215, 1982.
8. Fan, F.Y., Chiu, C.C., Tseng, C.L., Lee, H.S., Pan, Y.N., and Yang, K.C. Glycosaminoglycan/chitosan hydrogel for matrix-associated autologous chondrocyte implantation: an *in vitro* study. J Med Biol Eng **34,** 211, 2014.
9. Kretlow, J.D., Klouda, L., and Mikos, A.G. Injectable matrices and scaffolds for drug delivery in tissue engineering. Adv Drug Deliv Rev **59,** 263, 2007.
10. Huang, N.F., and Li, S. Regulation of the matrix microenvironment for stem cell engineering and regenerative medicine. Ann Biomed Eng **39,** 1201, 2011.
11. Badylak, S.F. Xenogeneic extracellular matrix as a scaffold for tissue reconstruction. Transpl Immunol **12,** 367, 2004.
12. Hutmacher, D.W. Scaffolds in tissue engineering bone and cartilage. Biomaterials **21,** 2529, 2000.
13. Kharkar, P.M., Kiick, K.L., and Kloxin, A.M. Designing degradable hydrogels for orthogonal control of cell microenvironments. Chem Soc Rev **42,** 7335, 2013.
14. Liu, X., and Ma, P.X. Polymeric scaffolds for bone tissue engineering. Ann Biomed Eng **32,** 477, 2004.
15. Temenoff, J.S., and Mikos, A.G. Review: tissue engineering for regeneration of articular cartilage. Biomaterials **21,** 431, 2000.
16. Chang, C.H., Kuo, T.F., Lin, F.H., Wang, J.H., Hsu, Y.M., Huang, H.T., *et al.* Tissue engineering-based cartilage repair with mesenchymal stem cells in a porcine model. J Orthop Res **29,** 1874, 2011.
17. Trattnig, S., Ba-Ssalamah, A., Pinker, K., Plank, C., Vecsei, V., and Marlovits, S. Matrix-based autologous chondrocyte implantation for cartilage repair: noninvasive monitoring by high-resolution magnetic resonance imaging. Magn Reson Imaging **23,** 779, 2005.
18. Wang, C.C., Yang, K.C., Lin, K.H., Wu, C.C., Liu, Y.L., Lin, F.H., *et al.* A biomimetic honeycomb-like scaffold prepared by flow-focusing technology for cartilage regeneration. Biotechnol Bioeng **111,** 2338, 2014.
19. Chiang, T.S., Yang, K.C., Zheng, S.K., Chiou, L.L., Hsu, W.M., Lin, F.H., *et al.* The prediction of drug metabolism using scaffold-mediated enhancement of the induced cytochrome P450 activities in fibroblasts by hepatic transcriptional regulators. Biomaterials **33,** 5187, 2012.
20. Frisbie, D.D., Cross, M.W., and McIlwraith, C.W. A comparative study of articular cartilage thickness in the stifle of animal species used in human pre-clinical studies compared to articular cartilage thickness in the human knee. Vet Comp Orthop Traumatol **19,** 142, 2006.
21. Wang, L.S., Du, C., Toh, W.S., Wan, A.C., Gao, S.J., and Kurisawa, M. Modulation of chondrocyte functions and stiffness-dependent cartilage repair using an injectable enzymatically crosslinked hydrogel with tunable mechanical properties. Biomaterials **35,** 2207, 2014.
22. Yang, K.C., Chen, H.T., Wu, C.C., Lian Y.J., Chen, L.L., Sumi, S., *et al.* L-Glutamine regulates the expression of matrix proteins, pro-inflammatory cytokines and catabolic enzymes in IL-1β-stimulated human chondrocytes. Process Biochem **51,** 414, 2016.
23. Brittberg, M., Lindahl, A., Nilsson, A., Ohlsson, C., Isaksson, O., and Peterson, L. Treatment of deep cartilage defects in the knee with autologous chondrocyte transplantation. N Engl J Med **331,** 889, 1994.
24. O'Driscoll, S.W., Keeley, F.W., and Salter, R.B. Durability of regenerated articular cartilage produced by free autogenous periosteal grafts in major full-thickness defects in joint surfaces under the influence of continuous passive motion. A follow-up report at one year. J Bone Joint Surg Am **70,** 595, 1988.
25. Shao, X., Goh, J.C., Hutmacher, D.W/, Lee, E.H., and Zigang, G. Repair of large articular osteochondral defects using hybrid scaffolds and bone marrow-derived mesenchymal stem cells in a rabbit model. Tissue Eng **12,** 1539, 2006.
26. Hacker, S.A., Healey, R.M., Yoshioka, M., and Coutts, R.D. A methodology for the quantitative assessment of articular cartilage histomorphometry. Osteoarthritis Cartilage **5,** 343, 1997.
27. Pabbruwe, M.B., Esfandiari, E., Kafienah, W., Tarlton, J.F., and Hollander, A.P. Induction of cartilage integration by a chondrocyte/collagen-scaffold implant. Biomaterials **30,** 4277, 2009.
28. Peretti, G.M., Zaporojan, V., Spangenberg, K.M., Randolph, M.A., Fellers, J., and Bonassar, L.J. Cell-based bonding of articular cartilage: an extended study. J Biomed Mater Res **64A,** 517, 2003.
29. Peretti, G.M., Randolph, M.A., Caruso, E.M., Rossetti, F., and Zaleske, D.J. Bonding of cartilage matrices with cultured chondrocytes: an experimental model. J Orthop Res **16,** 89, 1998.
30. Tanaka, T., Komaki, H., Chazono, M., and Fujii, K. Use of a biphasic graft constructed with chondrocytes overlying a beta-tricalcium phosphate block in the treatment of rabbit osteochondral defects. Tissue Eng **11,** 331, 2005.
31. Zeifang, F., Oberle, D., Nierhoff, C., Richter, W., Moradi, B., and Schmitt, H. Autologous chondrocyte implantation using the original periosteum-cover technique versus matrix-associated autologous chondrocyte implantation: a randomized clinical trial. Am J Sports Med **38,** 924, 2010.
32. Wang, W., Tam, M.D., Spain, J., and Quintini, C. Gelfoam-assisted amplatzer vascular plug technique for rapid occlusion in proximal splenic artery embolization. AJR Am J Roentgenol **200,** 677, 2013.

33. Sanno, K., Hatanaka, N., Yamagishi, T., Nakazawa, I., Hirano, Y., Hosaka, K., *et al.* Selective gelfoam embolization of primary racemose haemangioma of the bronchial artery. Respirology **14,** 609, 2009.
34. Lee, J.W., Cuddihy, M.J., and Kotov, N.A. Three-dimensional cell culture matrices: state of the art. Tissue Eng Part B Rev **14,** 61, 2008.
35. Khan, I.M., Gilbert, S.J., Singhrao, S.K., Duance, V.C., and Archer, C.W. Cartilage integration: evaluation of the reasons for failure of integration during cartilage repair. A review. Eur Cell Mater **16,** 26, 2008.
36. Heir, S., Årøen, A., Løken, S., Sulheim, S., Engebretsen, L., and Reinholt, F.P. Intraarticular location predicts cartilage filling and subchondral bone changes in a chondral defect. Acta Orthop **81,** 619, 2010.

Address correspondence to:
Tzong-Fu Kuo, PhD
Graduate Institute of Veterinary Medicine
School of Veterinary Medicine
National Taiwan University
No. 1, Sec. 4, Roosevelt Road
Taipei 10617
Taiwan

E-mail: tzongfu@ntu.edu.tw

Ing-Ho Chen, MD
Department of Orthopedics
School of Medicine
Tzu Chi University
No. 707, Sec. 3, Chung Yang Road
Hualien 97004
Taiwan

E-mail: ing.ho@msa.hinet.net

Received: November 9, 2015
Accepted: May 16, 2016
Online Publication Date: June 1, 2016